NANO LETTERS

2007
Vol. 7, No. 2
323−328

Rational Synthesis of p-Type Zinc Oxide Nanowire Arrays Using Simple Chemical Vapor Deposition

Bin Xiang,[†] Pengwei Wang,[‡] Xingzheng Zhang,[‡] Shadi. A. Dayeh,[†] David P. R. Aplin,[†] Cesare Soci,[†] Dapeng Yu,[‡] and Deli Wang*[,†]

Department of Electrical and Computer Engineering, University of California at San Diego, La Jolla, California 92093-0407, and Electron Microscopy Laboratory, School of Physics, Peking University, Beijing 100871, China

Received October 13, 2006; Revised Manuscript Received December 8, 2006

ABSTRACT

We report, for the first time, the synthesis of the high-quality p-type ZnO NWs using a simple chemical vapor deposition method, where phosphorus pentoxide has been used as the dopant source. Single-crystal phosphorus doped ZnO NWs have their growth axis along the ⟨001⟩ direction and form perfect vertical arrays on *a*-sapphire. P-type doping was confirmed by photoluminescence measurements at various temperatures and by studying the electrical transport in single NWs field-effect transistors. Comparisons of the low-temperature PL of unintentionally doped ZnO (n-type), as-grown phosphorus-doped ZnO, and annealed phosphorus-doped ZnO NWs show clear differences related to the presence of intragap donor and acceptor states. The electrical transport measurements of phosphorus-doped NW FETs indicate a transition from n-type to p-type conduction upon annealing at high temperature, in good agreement with the PL results. The synthesis of p-type ZnO NWs enables novel complementary ZnO NW devices and opens up enormous opportunities for nanoscale electronics, optoelectronics, and medicines.

Zinc oxide (ZnO) is a wide direct band gap semiconductor ($E_g = 3.4$ eV) that displays unique features such as large exciton binding energy ($E_b = 60$ meV)[1] and large piezoelectric and ferromagnetic coefficients with a predicted Curie temperature above room temperature when doped with transition metals.[2,3] The availability of a rich genre of nanostructures[4−6] make ZnO an ideal material for nanoscale optoelectronics,[7] electronics,[8,9] and biotechnology.[10] Functional devices such as vertical nanowire (NW) FETs,[9] piezoelectric nanogenerators,[11,12] optically pumped nanolasers,[7,13] and biosensors[10] have already been demonstrated. However, similar to other wide band gap semiconductors such as GaN,[14] unintentionally doped ZnO is intrinsically n-type and obtaining p-type doping[15] has proven extremely difficult. Although p-type conduction in ZnO thin film has been reported, it still remains controversial,[1,16] and no report of p-type ZnO NWs has appeared yet.[8,9,17] Complementary doping (both n-type and p-type doping) is essential for functional device applications, and the lack of p-type ZnO NWs is currently the major factor precluding the realization of a wide range of functional nanodevices based on ZnO. Herein we report the first demonstration and rational synthesis of the high-quality p-type ZnO NWs using a simple chemical vapor deposition (CVD) method using phosphorus pentoxide (P_2O_5) as the dopant source. P-type doping was confirmed by photoluminescence (PL) measurements at various temperatures and by studying the electrical transport in single NWs field-effect transistors (FETs). The synthesis of p-type ZnO NWs enables novel complementary ZnO NW devices and circuits,[9] UV-LEDs, and electrically driven nanolasers,[18] multiplexing biosensors,[19] etc., and opens up enormous opportunities for nanoscale electronics, optoelectronics, and medicines.

The ZnO:P NWs are grown using a simple tube furnace CVD method through chemical vapor deposition, with an O_2/N_2 mixture as the carrier gas.[20] A mixture of ZnO powder (99.999% from Cerac), Zn powder, graphite powder (mesh size of 200 from Alfa Aesar) with a molar ratio of 1:1 ZnO/C, and P_2O_5 powder was used as the source. The source was loaded in an Al_2O_3 boat, which was set at the center of the tube furnace (Lindberg-Blue). *A*-plane sapphire was cleaned using a standard wafer cleaning procedure and set to a fixed distance (4.75 in.) downstream from the source boat. A mixture of nitrogen and oxygen (3 sccm) with a total flow rate of 200 sccm was used as a carrier gas. The growth was performed at 945 °C for 30 min. The growth procedure for unintentionally doped ZnO NWs was similar to that of ZnO:P NWs, but a mixture of ZnO and graphite powder only

* Corresponding author. E-mail: dwang@ece.ucsd.edu.
[†] Department of Electrical and Computer Engineering, University of California at San Diego.
[‡] Electron Microscopy Laboratory, School of Physics, Peking University.

10.1021/nl062410c CCC: $37.00
Published on Web 12/29/2006

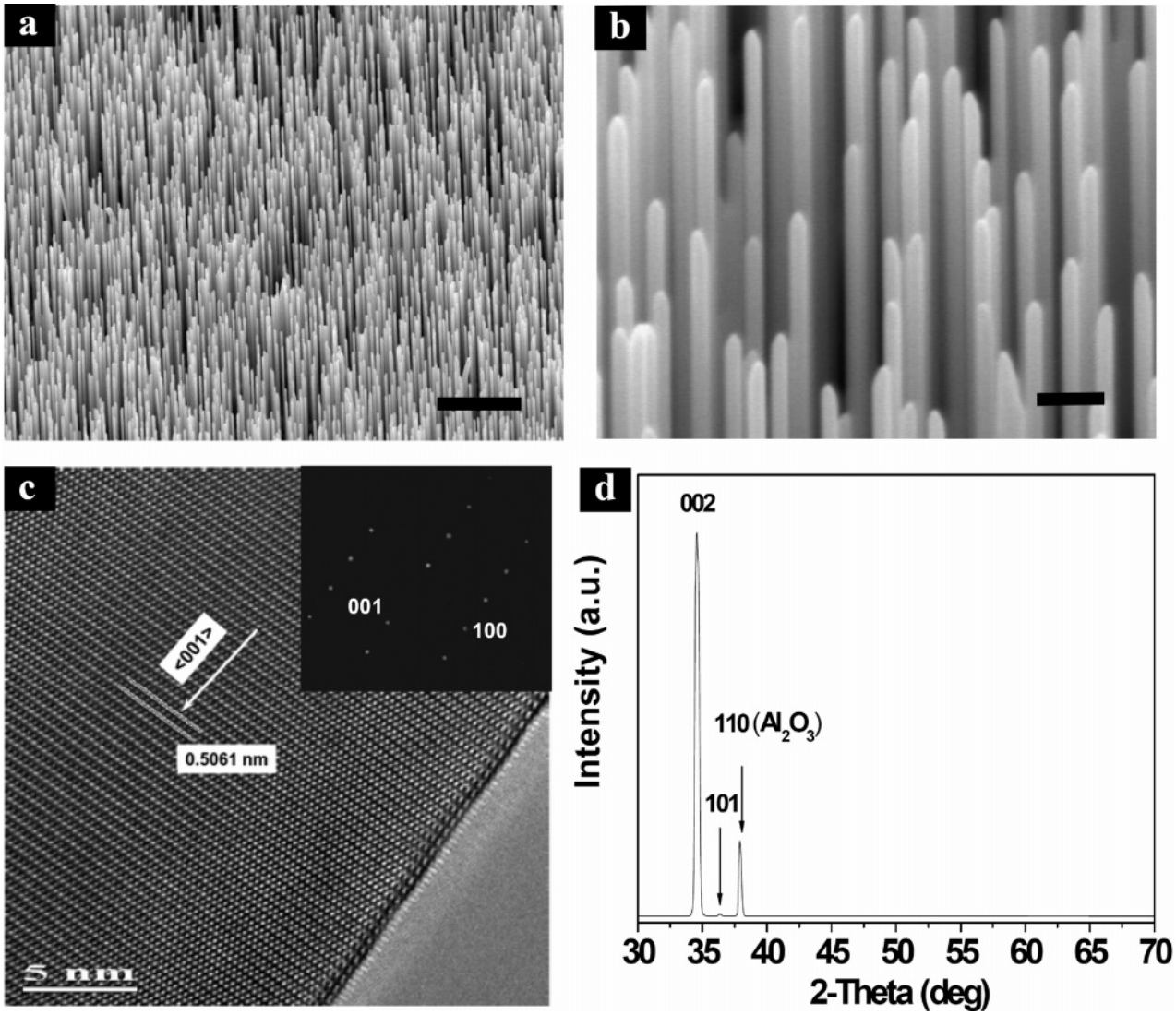

Figure 1. Structural and morphological characterization of the ZnO:P NWs. (a) Low-magnification SEM image of the well-oriented ZnO:P NW arrays. Scale bar is 2 μm. (b) High-magnification SEM image of the ZnO:P NW arrays, showing that the NWs have uniform diameters (~55 nm) and very smooth surfaces. Scale bar is 200 nm. (c) HRTEM image of ZnO:P NWs showing high-quality single crystal with extremely clean and smooth surface; note the absence of any amorphous layer coating on the surface. The electron diffraction pattern is shown in the inset, from which no second phase or cluster could be detected. The growth direction is along ⟨001⟩ direction as indexed in the images. (d) XRD spectrum of the ZnO:P NWs treated by RTA. The typical X-ray diffraction pattern of ZnO NW arrays is observed, with no peaks associated to second phases or clusters.

(molar ratio 1:1) and nitrogen only (200 sccm) were used as the source and carrier gases, respectively.

The phosphorus-doped ZnO NW vertical arrays were grown on an *a*-plane sapphire substrate. Figure 1a shows a representative field emission scanning electron microscopy (FE-SEM) image of vertical ZnO NW arrays on *a*-plane sapphire. Vertical NW arrays covering large areas of the substrate (4 mm × 6 mm) have been reproducibly accomplished. For a growth time of 30 min, the as-grown ZnO:P NWs show very uniform diameters (between 50 and 60 nm) and length (~2 μm) and morphologically smooth surfaces, which are significantly thinner and longer compared to the unintentionally doped ZnO NWs grown under similar conditions (Figures 1b, S1a, and S1b). These ZnO:P NWs are slightly tapered at the NW tips. Increasing the P_2O_5 weight percentage in the source mixture results in sharp tapering of the NWs (for example, see the SEM images of tapered NWs grown with 30% of P_2O_5 in weight in Figure S1c).

Carbon has been used to reduce P_2O_5 into P vapor during the elemental phosphorus production[21] according to the following reaction:

$$P_2O_5\,(s) + 5C\,(s) = 2P\,(g) + 5CO\,(g) \qquad (1)$$

We believe that, in our experiments, carbon simultaneously reduces ZnO and P_2O_5 into Zn and P vapors, respectively, which as clusters (P_4 or Zn_3P_2) are carried to the sapphire substrate placed downstream; P_2O_5 will also be present because of its high vapor pressure.[22] Both Zn_3P_2 and P_2O_5 are possible dopants[1,20] and are incorporated in ZnO NWs during the growth. The Zn−P bond length (2.18 Å) is

significantly larger than that of the Zn−O bond (1.93 Å), therefore, P atoms introduce lattice strain when they occupy the substitutional oxygen sites. P atoms tend to sit in the Zn sites of the lattice and form donorlike antisites, P_{Zn}.[1,15] The P_{Zn}−O bonding has a smaller bonding length (1.68 Å) on the *c*-axis and similar bonding length (1.60 Å) off the *c*-axis for the ionized P_{Zn} donors, and therefore P_{Zn} defects will also introduce strain to the ZnO lattice. The strain relaxes along the radial direction of the one-dimensional nanowires and the relaxation increases with decreasing diameter.[23] The smaller diameters of ZnO:P NWs with respect to the unintentionally doped ZnO NWs and their tapered morphology suggest uniform P incorporation into the ZnO NW bodies rather than on the surface layers only.

High-resolution transmission electron microscopy (HR-TEM) images show atomically resolved wurzite ZnO single crystal after annealing, as shown in Figure 1c. The growth axis is along the ⟨001⟩ direction, which is confirmed by the select area electron diffraction (SAED) analysis (Figure 1c inset). The spacing between *c*-ZnO:P planes is 5.035 Å and is significantly smaller than that in intrinsic ZnO NWs (5.2 Å)[24] and in ZnO thin film (5.207 Å),[1] which indicates the lattice compression due to the P doping and possibly the presence of P_{Zn} defects. The ZnO:P NWs have perfectly smooth surfaces without any amorphous coating (Figure 1c) and extremely uniform diameter, which gradually reduces to about 5 nm at the tip with a tapering length of around 50 nm (Figure S1). The X-ray diffraction (XRD) pattern shows a strong and sharp peak from the (002) plane and further confirms the high quality of single-crystal ZnO:P NWs with the growth axis along the *c*-direction. Energy dispersive X-ray microanalysis (EDX) has detected only Zn and O within the detection limits (Figure S2a), and X-ray photoelectron spectroscopy (XPS) analysis has shown that only the ZnO phase is obtained, indicating that the ZnO:P NWs do not contain secondary phases or clusters and suggesting atomic level incorporation of the dopant.

The photoluminescence (PL) study[25] of ZnO:P NWs after annealing in N_2 gas at 850 °C for 1 min with N_2 gas flow of 25 slm shows a very strong emission at 3.352 eV with FWHM of 30 meV at room temperature (Figure 2a), which is attributed to the band edge emission of ZnO NWs. The broad, weak red emission centered at 1.8 eV indicates the absence of oxygen vacancy levels that are responsible for the typical green emission in ZnO thin film and nanomaterials.[1] The nature of the red emission from P-doped ZnO has not been reported in the literature. We anticipate that it is due to the radiative recombination of ionized donors and acceptors (please see discussion in the Supporting Information, Figure S4). The weak red emission is significantly quenched at low temperature and completely disappears at 10 K (Figure 2a), further suggesting that it originates from the ionized dopants. The peaks between 1.67 and 1.69 eV are believed to be the second-order peaks of the excitonic emission (please see the Supporting Information). For comparison, we have also performed temperature-dependent PL measurements on the as-grown ZnO:P NWs (before annealing) (Figure 2b) and unintentionally doped ZnO NWs

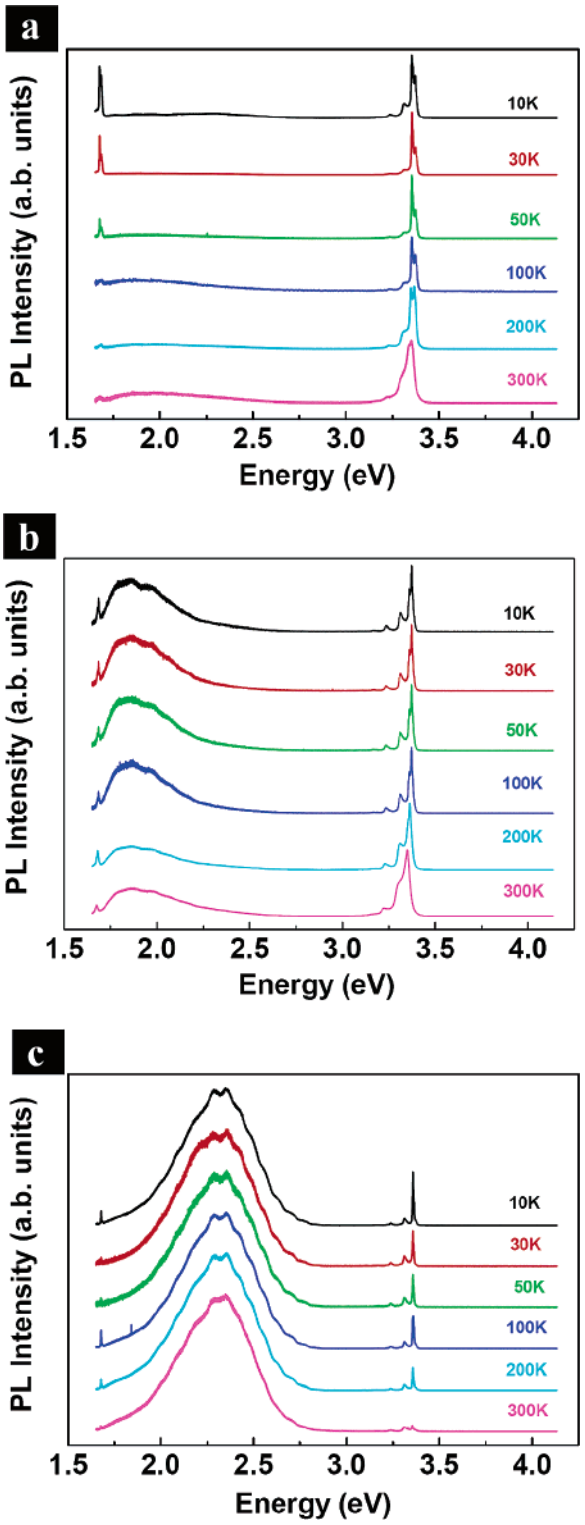

Figure 2. PL spectra of the as-grown ZnO NWs. (a) Temperature dependence of the PL spectra of thermally annealed ZnO:P NWs in the temperature range of 10−300 K. (b) Temperature-dependent PL spectra (10−300 K) of as-grown ZnO:P NWs. (c) Temperature-dependent PL spectra of n-type ZnO NWs from 10 to 300 K.

(Figure 2c). The room-temperature PL of the as-grown ZnO:P NWs shows a strong PL emission at 3.35 eV with FWHM of 20 meV and a relatively stronger red emission compared to that from annealed ZnO:P NWs (Figure 2a). Again, no green emission associated to V_O was observed in

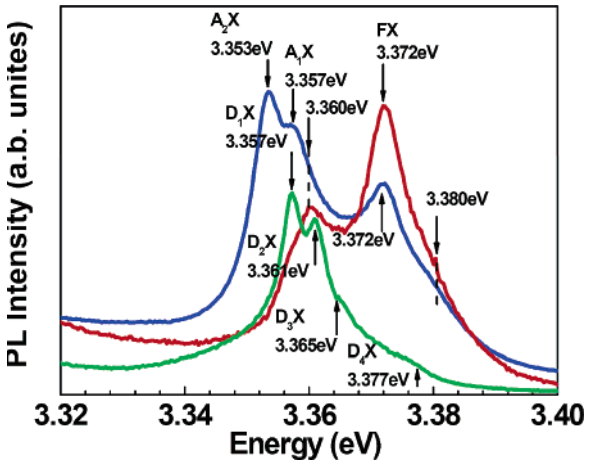

Figure 3. Excitonic peaks of PL spectra at 10K of n-type (green line), as-grown (red line), and annealed (blue line) ZnO:P NWs.

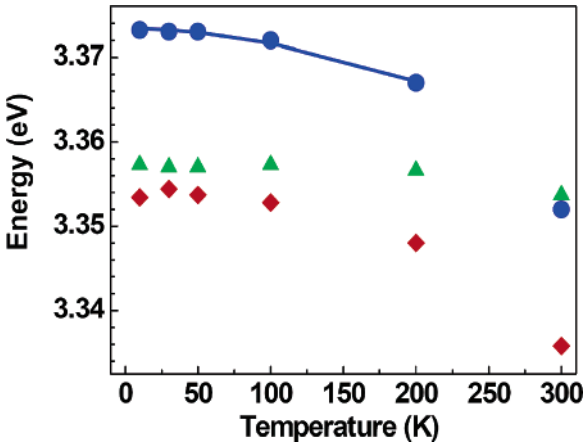

Figure 4. Temperature dependence of the transition energy of the FX (blue dots), DX (green triangles), and AX (red diamonds) from the photoluminescence peaks of the annealed, unintentionally doped, and as-grown ZnO:P NWs, respectively. The blue line is the corresponding fitting curve derived from the Varshni equation.

as-grown ZnO:P NWs. On the other hand, the room-temperature PL spectra from ZnO:P NWs are very different from those of the unintentionally n-doped ZnO NWs, as shown in Figures 2c and S4a. The PL from n-type ZnO NWs shows very weak band-edge emission in the UV, but strong and broad visible emission centered at 2.36 eV, which is due to oxygen vacancies.[1]

Low-temperature PL studies reveal fine excitonic emission from the ZnO NWs and the comparison between the unintentionally doped, as-grown ZnO:P, and annealed ZnO:P NWs unambiguously indicated the p-doping, as shown in Figures 3, S4b, and S4d, respectively. At 10 K, this strong UV emission from the annealed ZnO:P NWs is structured into fine bands due to the free exciton peaks, FX_A (3.372 eV) and FX_B (3.380 eV), and two neutral acceptor-bound excitons, $A^0{}_1X_A$ (3.357 eV) and $A^0{}_2X_A$ (3.353 eV), while the $A^0{}_2X$ is the strongest peak with a FWHM of 2.2 meV (blue line in Figure 3).[26] The red line in Figure 3 shows the low-temperature PL of the as-grown ZnO:P NWs, which shows free exciton levels, FX_A (3.372 eV) and FX_B (3.380 eV), and one neutral donor-bound exciton level, D_0X (3.360 eV)). The FX_A is the strongest peak that has a FWHM of 4.8 meV. The ZnO:P NWs are significantly different from the n-doped ZnO NWs, which, as shown by the low-temperature PL (green line in Figure 3), has only neutral donor-bound exciton peaks, $D^0{}_1X_A$ (3.357 eV), $D^0{}_2X_A$ (3.361 eV), $D^0{}_3X_A$ (3.365 eV), and $D^0{}_4X_A$ (3.377 eV). The $D^0{}_1X_A$ is strongest and has a FWHM of 1.8 meV.

Figure 4 shows the exciton peaks evolution with temperature: the temperature dependence of free excitons (FX, blue dots), donor-bound excitons (DX, green triangles), and acceptor-bound excitons (AX, red diamonds) from the photoluminescence peaks of the annealed, unintentionally doped, and as-grown ZnO:P NWs, respectively. The free exciton level was found to follow the Varshni formula[27] $E_g(T) = E_g(0) - \alpha T^2/(T + \beta)$, where $E_g(T)$ is the band gap energy, T is temperature (K), and α and β are the temperature coefficients. α and β were found to be 1×10^{-4} eV/K and 700 K, respectively.

The clear transition from the donor-bound exciton peak to acceptor-bound exciton peaks from ZnO:P NWs after the annealing process (Figure 3) agrees extremely well with the electrical measurement of ZnO NW back-gate field-effect transistors (FETs) at room temperature.[28] Figure 5a shows the output characteristics at various back-gate voltages (V_{GS}), and Figure 5b shows the gate sweep characteristic at $V_{DS} =$ 15 V of a typical ZnO:P NW with global n^+-Si back-gate (Figure 5b inset), which clearly indicates p-type conduction. The threshold voltage is about $V_{th} = -5$ V, as obtained from a linear extrapolation of the $I_{DS}-V_{GS}$ curve in Figure 5b. The field-effect mobility of the p-type ZnO nanowires can be calculated from $\mu_{FE} = g_m/(2\pi\epsilon\epsilon_0 L V_{DS}/\ln(2t/r))$,[29,30] where g_m is the transconductance, ϵ is the relative dielectric constant of the SiO_2 dielectric, L is the device channel length, and r is the NW radius. $g_m = dI_{DS}/dV_{GS}$ was obtained from the $I_{DS}-V_{GS}$ plot (Figure 5b) to be 0.1 μS (neglecting the contact resistance), corresponding to an estimated carrier mobility of $\mu_{FE} \sim 1.7$ cm^2/V·s, which is comparable to the reported results for p-type ZnO films with phosphorus dopants.[31,32] Please note this value represents the low bound limit of the hole mobility because no serial contact resistance at the metal/nanowire interface was considered. The same holds true for the electron mobility values discussed below for the unintentionally doped ZnO NWs and as-grown ZnO:P NWs. For a quasi-one-dimensional system, the hole concentration p can be estimated as $p = (V_{gt}/h) \times (2\pi\epsilon\epsilon_0/\ln(2t/r))$,[29,30] where t is the thickness of the oxide layer and r is the radius of the nanowire. The carrier concentration p is estimated to be $\sim 2.2 \times 10^7$ cm^{-1}. It has been suggested that, under O_2-rich growth conditions,[20] the formation of $[P_{Zn}-2V_{Zn}]$ complexes is more favorable than the formation of Zn vacancies, V_{Zn}, whose ϵ (1−/0) transition levels act as shallow acceptors compared to P_O^- acceptors[20] and are responsible for the excellent conductance and high hole concentration of P-doped ZnO. The existence of $[P_{Zn}-2V_{Zn}]$ complexes agrees well with the red emission observed in the PL studies (see discussion in Figure 4S).

The representative room temperature output and transconductance characteristics of single as-grown ZnO:P NW FETs fabricated identically clearly show n-type conductance, and

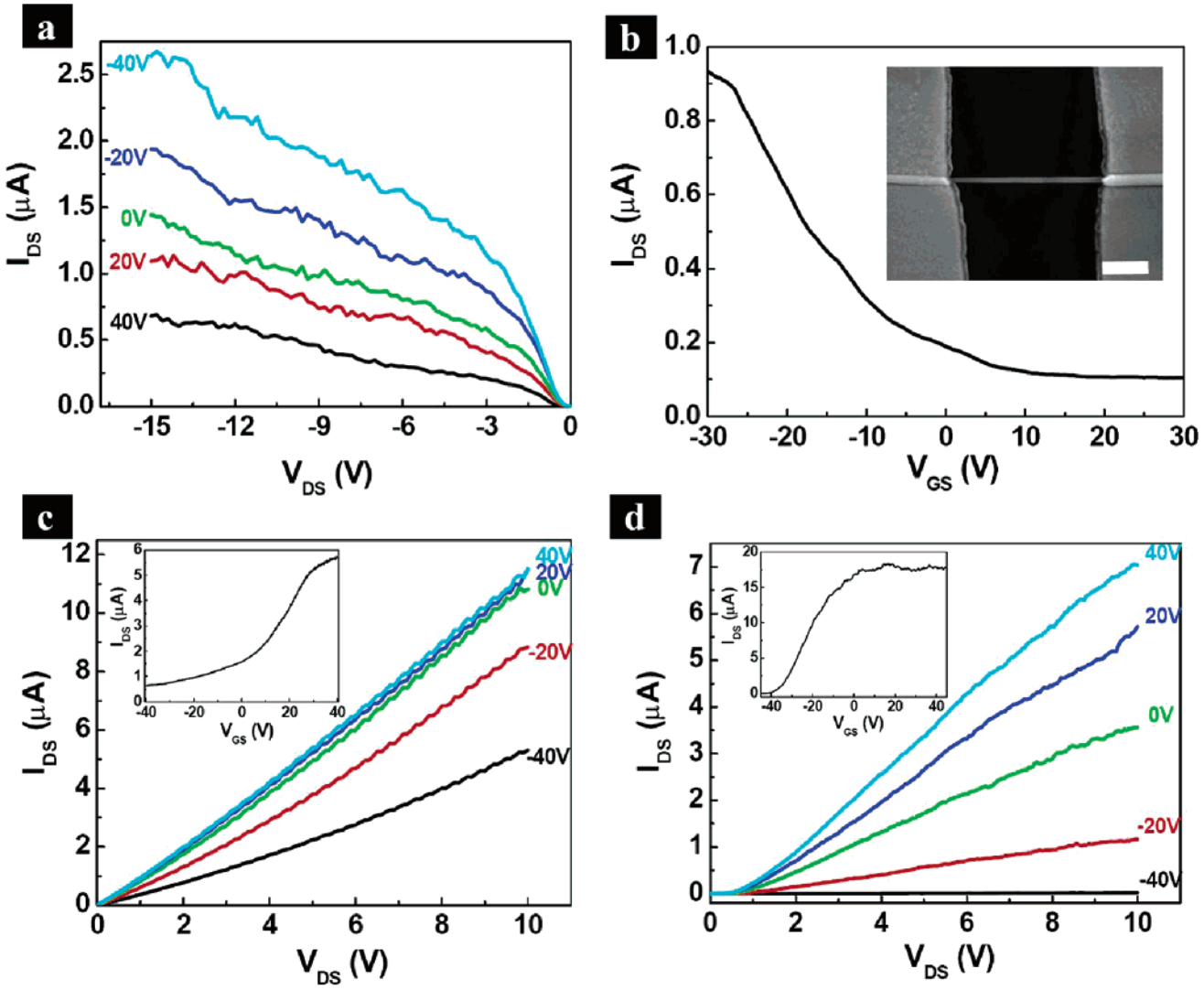

Figure 5. Characteristics of ZnO NW FETs. (a) $I_{DS}-V_{DS}$ plots of the ZnO:P NW treated by RTA transistor at different back-gate voltages. (b) $I_{DS}-V_{GS}$ plot of the annealed ZnO:P NWs transistor at $V_{DS} = 15$ V. Inset: SEM image of the measured device. The scale bar is 500 nm. (c) $I_{DS}-V_{DS}$ plots of the as-grown ZnO:P NW transistor at the different back-gate voltages. Inset: corresponding $I_{DS}-V_{GS}$ plot at $V_{DS} = 6$ V. (d) $I_{DS}-V_{DS}$ plots of the n-type ZnO NW transistor at different back-gate voltages. The corresponding $I_{DS}-V_{GS}$ plot at $V_{DS} = 15$ V is displayed in the inset.

the estimated electron concentration and mobility are 1.0×10^8 cm^{-1} and 2.2 cm^2/V·s, respectively. According to the above PL study, no oxygen vacancies should be present in ZnO:P NWs, therefore the n-type transport behavior is likely to arise from P_{Zn} antisites, which are donorlike and compensate P_O substitutional dopants.[15,20] On the other hand, the n-type behavior of unintentionally doped ZnO NWs is clearly related to oxygen vacancies, which is very well-known in the literature and confirmed by our PL study (Figure 2c) as well. Figure 5d shows the transistor characteristics of an n-type ZnO NW, from which we estimated a field-effect mobility value of 5.9 cm^2/V·s and a carrier concentration of 3.7×10^8 cm^{-1}. Note that the n-type ZnO NW device has a very large on/off ratio of about 10^7, while the on/off ratio of ZnO:P NWs devices with/without annealing are much lower (10 and 8, respectively). The p-type conductance from annealed ZnO:P NWs was found to be quite stable and persists for storage in air for more than 2 months before showing n-type behavior.

In summary, our study describes the first demonstration of high-quality single-crystal p-type ZnO NWs using P as the dopant, with growth axis in the ⟨001⟩ crystallographic orientation, by a simple CVD method. The NW growth is very reproducible and perfectly aligned vertical arrays on an *a*-sapphire substrate can be routinely achieved on fairly large areas. The room-temperature PL study of annealed ZnO:P NWs reveals a very strong sharp band edge emission at 3.35 eV, which is much stronger than that from unintentionally doped ZnO NWs. At low temperature, clear emission from a donor-bound exciton in unintentionally doped ZnO NWs from free- and donor-bound excitons in as-grown ZnO:P NWs and from free- and acceptor-bound excitons in annealed ZnO:P NWs were observed. No green photoluminescence from both as-grown and annealed ZnO:P NWs could be detected, indicating the absence of oxygen vacancies. A broad red emission was observed in ZnO:P NWs, although it was significantly quenched after thermal annealing. This red emission is effectively quenched at low

temperature in the annealed ZnO:P NWs. We have attributed the red emission to radiative recombination between donor and acceptor levels. The low-temperature PL studies agree extremely well with the transport studies; p-type conductance was observed in the annealed ZnO:P NWs, while both as-grown ZnO:P NWs and unintentionally doped ZnO NWs showed n-type behavior, although originating from different mechanisms. The success in rational p-doping of ZnO NWs enables enormous opportunities for nanoscale electronics, optoelectronics, and medicines. Furthermore, the p-doping of ZnO NWs could also allow achieving 1D diluted magnetic semiconductor (DMS) nanostructures with a Curie temperature higher than room temperature in the research area of carrier-mediated ferromagnetism.[33,34] Indeed, ferromagnetism has been theoretically predicted in 3D transition metal doped p-type, but not n-type, ZnO.[35]

Acknowledgment. We thank Mr. D. Scanderbeg for assistance in XPS and XRD measurement. D.W. acknowledges supports from the Office of Naval Research (ONR-Nanoelectronics), National Science Foundation (ECS-0506902), and Sharp Labs of America.

Supporting Information Available: SEM images of the Zno NWs synthesized with a different percentage of the P_2O_5 powder weight 0, 15, and 30%, respectively; HRTEM images of top of ZnO:P NWs; EDX and XPS analysis of the as-grown ZnO:P NWs (after annealing); photoluminescence studies of ZnO NWs. This material is available free of charge via the Internet at http://pubs.acs.org.

References

(1) Özgür, Ü.; Alivov, Y. I.; Liu, C.; Teke, A.; Reshchikov, M. A.; Doan, S.; Avrutin, V.; Cho, S.-J.; Morkoç, H. *J. Appl. Phys.* **2005**, *98*, 041301.
(2) Dietl, T.; Ohno, H.; Matsukura, F.; Cibert, J.; Ferrand, D. *Science* **2000**, *287*, 1019.
(3) Janisch, R.; Gopal, P.; Spaldin, N. A. *J. Phys.: Condens. Matter* **2005**, *17*, R657.
(4) Wang, Z. L. *J. Mater. Chem.* **2005**, *15*, 1021.
(5) Fan, H. J.; Werner, P.; Zacharias, M. *Small* **2006**, *2*, 700.
(6) Pan, Z. W.; Dai, Z. R.; Wang, Z. L. *Science* **2001**, *291*, 1947.
(7) Huang, M. H.; Mao, S.; Feick, H.; Yan, H. Q.; Wu, Y. Y.; Kind, H.; Weber, E.; Russo, R.; Yang, P. *Science* **2001**, *292*, 1897.
(8) Goldberger, J.; Sirbuly, D. J.; Law, M.; Yang, P. *J. Phys. Chem. B* **2005**, *109*, 9.
(9) Ng, H. T.; Han, J.; Yamada, T.; Nguyen, P.; Chen, Y. P.; Meyyappan, M. *Nano Lett.* **2004**, *4*, 1247.
(10) Wang, Z. L. *Annu. Rev. Phys. Chem.* **2004**, *55*, 159.
(11) Wang, Z. L.; Song, J. *Science* **2006**, *312*, 242.
(12) Song, J.; Zhou, J.; Wang, Z. L. *Nano Lett.* **2006**, *6*, 1656.
(13) Johnson, J. C.; Knutsen, K. P.; Yan, H. Q.; Law, M.; Zhang, Y. F.; Yang, P. D.; Saykally, R. J. *Nano Lett.* **2004**, *4*, 197.
(14) Morkoç, H.; Mohammad, S. N. *Science* **1995**, *267*, 51.
(15) Park, C. H.; Zhang, S. B.; Wei, S. H. *Phys. Rev. B* **2002**, *66*, 073202.
(16) Xia, Y. N.; Yang, P. D.; Sun, Y. G.; Wu, Y. Y.; Mayers, B.; Gates, B.; Yin, Y. D.; Kim, F.; Yan, Y. Q. *Adv. Mater.* **2003**, *15*, 353.
(17) Look, D. C.; Claflin, B.; Alivov, Y. I.; Park, S. J. *Phys. Status Solidi A* **2004**, *201*, 2203.
(18) Duan, X.; Huang, Y.; Agarwal, R.; Lieber, C. M. *Nature* **2003**, *421*, 241.
(19) Zheng, G.; Patolsky, F.; Cui, Y.; Wang, W. U.; Lieber, C. M. *Nat. Biotechnol.* **2005**, *23*, 1294.
(20) Lee, W. J.; Kang, J.; Chang, K. J. *Phys. Rev. B* **2006**, *73*, 024117.
(21) Massey, A. G. *Main Group Chemistry*, 2nd ed.; John Wiley & Sons: New York, 2000; p 286.
(22) www.jtbaker.com/msds/englishhtml/p4116.htm
(23) Ertekin, E.; Greaney, P. A.; Sands, T. D.; Chrzan, D. C. *Mater. Res. Soc. Symp. Proc.* **2003**, *737*, F10.4.1.
(24) Fan, H. J.; Fleischer, F.; Lee, W.; Nielsch, K.; Scholz, R.; Zacharias, M.; Gosele, U.; Dadgar, A.; Krost, A. *Superlattices Microstruct.* **2004**, *36*, 95.
(25) Room-temperature and low-temperature photoluminescence spectra of ZnO NWs were obtained using a Renishaw inVia Raman microscope with a He−Cd laser (325nm) as the light source. The samples were placed in a Janis closed-cycle refrigerator and cooled by liquid helium. The system was pumped to a pressure of $\sim 10^{-6}$ Torr using a turbomolecular pump. The laser beam was focused by a microscope objective normal to the substrate surface down to a spot size of around 1 μm in diameter. The laser power was 20 mW. The emitted light was dispersed by a 2400 mm^{-1} grating and detected by a $^1/_4$ in. format CCD with 3.2 mm $\times$ 2.4 mm slit size.
(26) Teke, A.; Özgür, Ü.; Doan, S.; Gu, X.; Morkoç, H.; Nemeth, B.; Nause, J.; Everitt, H. O. *Phys. Rev. B* **2004**, *70*, 195207.
(27) Wang, L.; Giles, N. C. *J. Appl. Phys.* **2003**, *94*, 973.
(28) The unintentionally doped (n-type), as-grown, and annealed ZnO:P NWs were transferred to an n^+-Si substrate with a 600 nm thermally grown SiO_2 layer (Nova Semiconductors). Ti/Au (20/160 nm) contact for n-type and as-grown ZnO:P NWs and Ni/Au (100/20 nm) contact for annealed ZnO:P NWs were defined by photolithography and consequently deposited using an E-beam evaporator. The devices were tested at room temperature using an HP4155 parameter analyzer.
(29) Martel, R.; Schmidt, T.; Shea, H. R.; Hertel, T.; Avouris, P. *Appl. Phys. Lett.* **1998**, *73*, 2447.
(30) Cui, Y.; Duan, X.; Hu, J.; Lieber, C. M. *J. Phys. Chem. B* **2000**, *104*, 5213.
(31) Kim, K.; Kim, H.; Hwang, D.; Lim, J.; Park, S. *Appl. Phys. Lett.* **2003**, *83*, 63.
(32) Xiong, G.; Wilkinson, J.; Mischuck, B.; Tuzemen, S.; Ucer, K. B.; Williams, R. T. *Appl. Phys. Lett.* **2002**, *80*, 1195.
(33) Choi, H. J.; Seong, H. K.; Chang, J.; Lee, K. I.; Park, Y. J.; Kim, J. J.; Lee, S. K.; He, R. R.; Kuykendall, T.; Yang, P. D. *Adv. Mater.* **2005**, *17*, 1351.
(34) Wang, Q.; Sun, Q.; Jena, P. *Phys. Rev. Lett.* **2005**, *95*, 167202.
(35) Sato, K.; Katayama-Yoshida, H. *Jpn. J. Appl. Phys.* **2000**, *39*, L555.

NL062410C